Energy 318 (2025) 134919

Contents lists available at ScienceDirect

Energy

journal homepage: www.elsevier.com/locate/energy

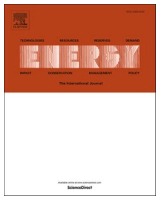

Kinetics simulation study of biomass partial gasification for producer gas and biochar co-production in the fluidized bed

Deao Zhu, Qinhui Wang *, Zijun Zhang, Guilin Xie, zhongyang Luo

State Key Laboratory of Clean Energy Utilization, Zhejiang University, Hangzhou 310027, China

ARTICLE INFO

Keywords:
Aspen plus
Biomass
Fluidized bed
Partial gasification
Co-production of producer gas and biochar
Kinetics simulation

ABSTRACT

Producer gas and biochar are the main products of biomass partial gasification in the fluidized bed. In order to reasonably predict the producer gas, biochar and performance indexes of biomass partial gasification process in the fluidized bed, a kinetic model considering tar reaction kinetics and biochar elements distribution of biomass partial gasification for producer gas and biochar co-production in bubbling fluidized bed was established by using Aspen plus, and the model are validated with the relevant experimental data under different air equivalence ratios. At the same time, the energy balance in the pyrolysis stage, oxidation stage and reduction stage of biomass partial gasification process in the bubbling fluidized bed under different air equivalence ratios was evaluated. The results indicate that the prediction data of producer gas components, biochar yield, gasification efficiency and carbon conversion ratio are in good agreement with the experimental data, and the root-mean-square error are less than 0.05. With the increase of air equivalence ratio(from 0.07 to 0.16), the gasification temperature keeps rising(from 602 °C to 716 °C), the volume contents of CO, CO_2 and C_nH_m keep decreasing, the volume contents of H_2 and CH_4 show an increasing-decreasing trend, and the volume content of N_2 keeps increasing; biochar yield continues to decline, the carbon and oxygen content in biochar decrease continuously; gasification efficiency and carbon conversion ratio keep increasing; the heat absorbing from the oxidation stage of the pyrolysis stage and reduction stage are increasing, and the heat releasing in the oxidation stage is also increasing.

1. Introduction

In order to help achieve the goal of carbon peak and carbon neutrality and national energy transition, biomass, as a renewable energy source with zero or even negative carbon emissions throughout its life cycle and huge development potential, has attracted much attention for its energy utilization. For raising energy utilization rate, reducing environmental pollution, optimizing the energy mix and accelerating green, low-carbon and circular development, it is imperative to have environment-friendly energy utilization technologies with large-scale handling capacity for agricultural and forestry waste.

Biomass gasification technology, known as a widely used, flexible, mature, economical, comprehensive, highly efficient and clean energy utilization technology, can change biomass into producer gas, biochar and tar through partial oxidation at high temperature (>500 °C) [1]. At present, the research methods of biomass gasification technology are mainly divided into experiment and simulation. Although the experimental methods are more intuitive and reliable, the simulation methods can save time and cost because it is not limited by experimental conditions and experimental equipment. At the same time, the simulation methods can play a key role in predicting the performance of gasification system and the design and optimization of gasifier. Therefore, much attention has been paid to study biomass gasification technology by means of simulation [2,3].

Currently, Aspen plus, Aspen HYSYS, ANSYS, Barracuda and Open Foams are the main simulation tools of biomass gasification technology [4–6]. ANSYS, Barracuda and Open Foams are based on Computational Fluid Dynamics (CFD) method for process simulation, focusing on fluid dynamics and mass and heat transfer within gasification systems. This method has been used in a large number of literatures [7–10], and its main challenges are the high computational power requirements and the accurate calculation of the physical properties of compounds under different conditions [3,11]. Aspen plus are based on the mass and energy conservation equations in combination with the phase equilibrium databases for process simulation. It is widely used for biomass gasification simulation because it has a complete physical property database and can

* Corresponding author.
E-mail address: qhwang@zju.edu.cn (Q. Wang).

https://doi.org/10.1016/j.energy.2025.134919
Received 4 November 2024; Received in revised form 15 January 2025; Accepted 6 February 2025
Available online 7 February 2025

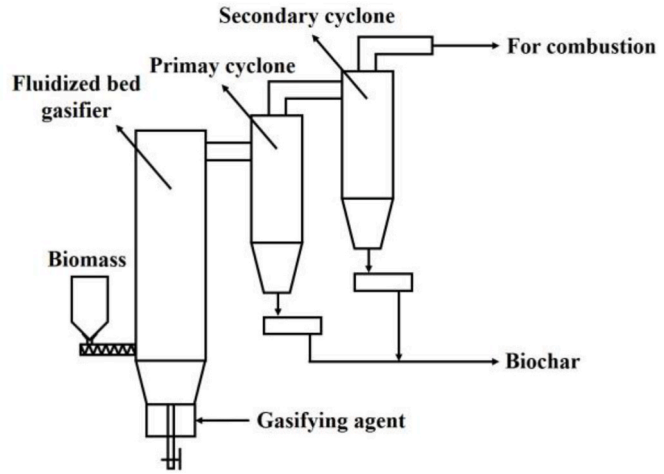

Fig. 1. Technical roadmaps for relevant technologies of biomass partial gasification for producer gas and biochar co-production in the fluidized bed.

flexibly use different unit operation modules to build complete process flow for simulation and optimization [12,13]. According to different simulation methods, Aspen plus for biomass gasification simulation can be divided into equilibrium and kinetics methods. The equilibrium method is relatively simple, generally using the Gibbs reactor module, which only considers the thermodynamic equilibrium and does not take into account the kinetics characteristics of the reaction. Furthermore, it is not suitable for low-temperature conditions and cannot provide satisfactory prediction results for the producer gas composition (especially C_nH_m). The kinetics method needs to consider the gasification reaction and kinetics characteristics involved, generally using the RCSTR kinetic reactor module or RPlug kinetic reactor module, which is more complicated but can get the results close to the experimental data even at low temperature [14,15]. Therefore, in order to achieve reasonable and accurate results, more and more literatures have adopted kinetics methods to simulate the biomass gasification process. Th. Damartzis [16] et al. developed a model for biomass gasification in bubbling fluidized bed using Aspen plus by integrating the kinetics of the homogeneous reactions, the non-homogeneous reactions and the tar oxidation reaction, and the results showed that the model fitted well with the experimental results obtained from the pilot plant and was able to give reliable predictions for the cold gas efficiency and thermal efficiency from air gasification of a wide variety of biomass. Priyanka Kaushal [17] et al. established a new biomass gasification model defining tar and its reaction kinetics in Aspen plus in view of the fact that tar was basically not considered in the existing biomass gasification simulation or tar was regarded as an inert substance. The results indicated that the accuracy and prediction performance of the model can be significantly improved by considering the tar and its kinetics reaction characteristics. Weiwei Li [18] et al. developed two models for waste tire gasification in bubble fluidized bed based on thermodynamic equilibrium method and kinetics method respectively, and the results demonstrated that the prediction performance of the kinetics model was significantly better than the thermodynamic equilibrium model, and the increase of temperature was conducive to reducing the difference between the two models in prediction for the producer gas composition and the lower heat value.

However, traditional biomass gasification aims for more valuable producer gas, paying more attention to the producer gas and related subsequent utilization, and focusing little on the biochar [19]. In recent years, the trend of value-added utilization of biochar has been obvious, and it has been widely used in many aspects [20]. Based on this, Zhejiang University put forward the relevant technology of biomass partial gasification for producer gas and biochar co-production in the fluidized bed to obtain high quality biochar and improve the economic feasibility of biomass energy utilization. The relevant technologies include biomass partial gasification in fluidized bed coupled with coal-fired power generation coproducing biochar (the industrial plant is under construction) and biomass partial gasification for steam and biochar co-production in fluidized bed (the industrial application has been realized), whose technology roadmaps are shown in Fig. 1 below. Therefore, it is necessary to conduct simulation research on the technology of biomass partial gasification for producer gas and biochar co-production to optimal operation and further improve the utilization value and economical efficiency of biomass.

Wajeha Tauqir [21] et al. developed a steady-state model for biomass gasification in the downdraft fixed bed using Aspen plus, in which the downdraft fixed bed was divided into four main regions to predict the effects of air equivalence ratio, gasification temperature and moisture content on producer gas and biochar production. The results revealed that when the air equivalence ratio was 0.14 and the gasification temperature was 750 °C, the cold gas efficiency reaches the highest, and the biochar yield decreases with the increase of air equivalence ratio, gasification temperature and moisture content. Zhiyi Yao [22] et al. constructed a comprehensive fixed-bed gasification model to predict the impact of air equivalence ratio on the yield and quality of producer gas and biochar in the fixed-bed gasification process, as well as the overall economic benefits of producer gas and biochar co-production. The results suggested that when the air equivalence ratio was 0.1, the higher heating value of producer gas was 6.15 MJ/Nm^3 and the highest biochar yield could reach 22 %. When the air equivalence ratio is 0.25, the maximum overall economic benefit was 0.11 $/kg. Yanping Zhou [23] used a kinetic method to simulate the downdraft fixed-bed gasification for producer gas and biochar cogeneration in Aspen plus, and the results indicated that with the increase of gasification temperature and air equivalence ratio, the gas production rate increased and the biochar yield decreased, and the highest biochar yield were 9.64 % and 10.31 %, respectively. However, the above simulation studies on biomass partial gasification for producer gas and biochar coproduction are mostly based on the fixed bed and biochar only consists of carbon and ash, so there is a lack of relevant simulation studies based on the fluidized bed and considering the elements distribution of biochar.

Therefore, in this paper, the kinetics simulation of biomass partial gasification for producer gas and biochar coproduction in the bubbling fluidized bed (BFB) was carried out by using Aspen plus on the basis of considering the tar reaction kinetics and the elements distribution of biochar, in which the kinetic parameters are determined based on the experimental results of biomass partial gasification for producer gas and biochar coproduction in BFB. At the same time, the effects of different air equivalence ratios on the characteristics of biomass partial gasification for producer gas and biochar coproduction and energy balance were analyzed, so as to provide corresponding data reference for industrial design and operation optimization of relevant technologies based on biomass partial gasification for biochar and producer gas coproduction in the fluidized bed.

Table 1
The proximate and ultimate analysis and lower heat value of poplar sawdust.

Ultimate Analysis/(wt%)					Proximate Analysis/(wt%)				$Q_{net,ad}$
C_{ad}	H_{ad}	N_{ad}	$S_{t,ad}$	O^*_{ad}	M_{ad}	A_{ad}	V_{ad}	FC_{ad}	MJ/kg
48.20	5.64	0.21	1.64	40.06	2.92	1.33	80.76	14.99	20.25

Note: ad: air dried basis. *: by subtraction.

Table 2
Operating conditions.

Operating conditions	1	2	3	4	5
ER	0.07	0.09	0.12	0.14	0.16
T/°C	602	634	673	689	716

2. Materials and methods

2.1. Biomass material

In order to verify with the experimental results related to biomass partial gasification for producer gas and biochar coproduction in the fluidized bed, the biomass feedstock selected for the simulation was poplar sawdust with good energy production potential, the same as in the experiments. And the results of its proximate and ultimate analysis and calorific value analysis are given in Table 1.

2.2. Experimental system

In this work, a self-built small atmospheric bubbling fluidized bed reactor was used to generate total product data to determine kinetics parameters and validate kinetics model. The experimental system and experimental methods are described in detail in Ref. [24]. Table 2 lists the experimental operating conditions of biomass partial gasification for producer gas and biochar in the bubbling fluidized bed.

2.3. Model introduction

The process of biomass partial gasification for producer gas and biochar co-production in the bubbling fluidized bed is very complex, which is generally considered to be composed of three processes: pyrolysis, oxidation combustion and gasification reduction. From the perspective of energy, in the process of biomass partial gasification for producer gas and biochar co-production in the bubbling fluidized bed, oxidation combustion stage provides the heat required for pyrolysis stage and gasification reduction stage. Therefore, the simulation process is divided into three successive sub-processes: pyrolysis, oxidation and reduction.

In addition, the bubbling fluidized bed reactor contains dense-phase and lean-phase regions, and the oxidation combustion reaction occurs in the dense phase region, the gasification reduction reaction occurs in the lean phase region. The RCSTR reactor module can simulate the multi-phase system, deal with the kinetics reaction with the solids, and can more realistically simulate the gasification reaction of the fluidized bed reactor. Therefore, from the viewpoint of simplifying the problem and directly using the built-in algorithm in Aspen Plus, two RCSTR reactor modules are connected in series and the corresponding reaction kinetics are defined to simulate the dense phase zone and lean phase zone for the gasification process in the bubbling fluidized bed. At the same time, according to the characteristics of uniform temperature of the fluidized bed reactor and same temperature of each phase of the RCSTR, the temperature of the two reactor modules are set the same, which is different from the fixed-bed reactors with obvious temperature zones and reaction zones. The specific model is shown in Fig. 2 below. In the model, CO、CO_2、CH_4、C_2H_4、H_2、H_2O、O_2、N_2、NO、NO_2、SO_2、SO_3、C_6H_6、C_7H_8、$C_{10}H_8$、C_6H_6O and $C_3H_6O_2$ are defined as conventional components, C and S are defined as solids, and biomass, char and ash are defined as unconventional components. The PR-BM method including Peng-Robinson and Boston Mathias functions is chosen as the physical property method.

In this model, Biomass was fed into a pyrolysis unit replaced by a RStoic reactor module under ambient conditions (25 °C and 1 atm), and its mass flow rate is constant. In the pyrolysis unit, the biomass was decomposed into several pyrolysis products, including pyrolysis gas, char and tar, using an numerical pyrolysis model. The Separator module (SEP) separates the pyrolysis products into char and volatile components, including pyrolysis gas and tar. Char is decomposed into C, H_2, O_2, N_2, S and ash by the Rstoic reactor module. In order to accurately simulate the element distribution of biochar under different air equivalent ratios, the Separator module(SEP-2) separates part of the H_2, O_2, N_2, S in the char decomposition products according to the ultimate analysis data obtained in the experiment and the calculated element residual rate, so that they did not participate in the reaction to became the H, O, N and S residues in biochar. The volatiles, char decomposition components involved in the reaction and ash, as well as AIR under ambient conditions (25 °C and 1 atm), were mixed in the Mixer module and sent to the oxidation unit replaced by a RCSTR kinetic reactor module, where the corresponding kinetic parameters are inputted to carry out the reaction. After the reaction is completed, the products are

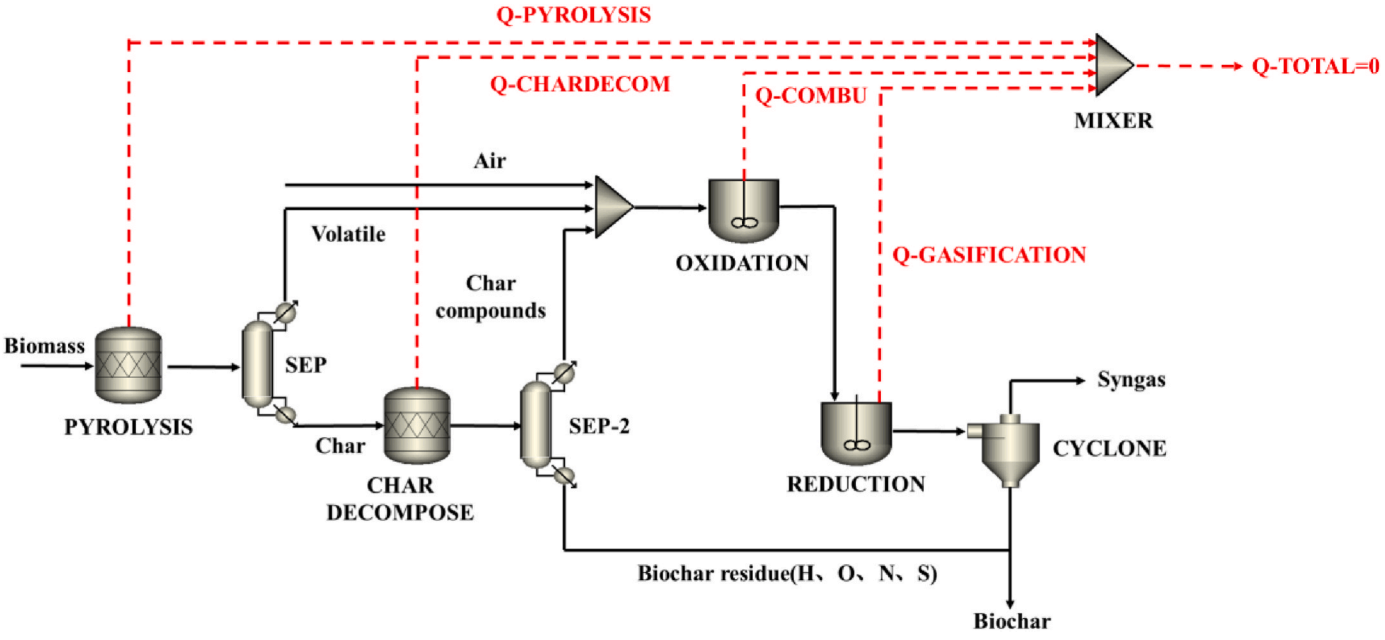

Fig. 2. Aspen plus model of biomass partial gasification for producer gas and biochar co-production in the fluidized bed.

sent into the reduction unit replaced by another RCSTR kinetic reactor module. The corresponding reaction kinetics parameters are input into the reduction unit for the final reduction reaction of gasification, and the gasification products is separated into producer gas and biochar by the Cyclone module so as to realize the producer gas and biochar coproduction of biomass partial gasification in the bubbling fluidized bed. In the model, the temperature of each reactor module is the same and consistent with the experiment [24]. Besides, the determination of air equivalence ratio consistent with the experiment and the energy balance in the whole process are realized by changing the initial value of the air volume flow to achieve process convergence. The tolerance is set to 0.001, and when the error between the input and output of the mass and energy for every module is less than the tolerance, the process will not report an error and converge.

In the simulation, the following assumptions are made: (1) The process is in steady, isothermal and atmospheric pressure state; (2) The pressure in the reactor is uniform, and there is no pressure and heat loss; (3) The drying of biomass and precipitation of volatiles are two independent one-step processes that occur instantaneously; (4) All gaseous compounds are ideal gases; (5) The composition of pyrolysis products is only related to temperature; (6) The gas components of the pyrolysis products do not take into account the substances containing S and N; (7) Unconverted carbon exists in the gasification process; (8) Tar is composed of C_6H_6, C_7H_8, $C_{10}H_8$, C_6H_6O and $C_3H_6O_2$; (9) Ash is inert.

2.3.1. Numerical pyrolysis model

In order to achieve reasonable and accurate simulation results, the empirical prediction model of pyrolysis products proposed by Daniel Neves [25] et al. was used to decompose biomass into H_2, CO, CO_2, CH_4, H_2O, C_nH_m, tar and char during the simulation process, in which C_nH_m was replaced by C_2H_4. The empirical prediction model is based on element balance and total gas energy balance, so as to ensure the mass balance, as shown in the matrix equation (1) for details. And in order to ensure that the model has a solution, the temperature empirical correlation formula is introduced, see equations (2)–(12) below, and the matrix equation is solved by Python. The empirical pyrolysis model was established by collecting and processing the pyrolysis products data of more than 60 different biomasses from different reactors under inert atmosphere and wide temperature range (200°C–1000 °C), so it can be used as a submodel to simulate different biomass gasification.

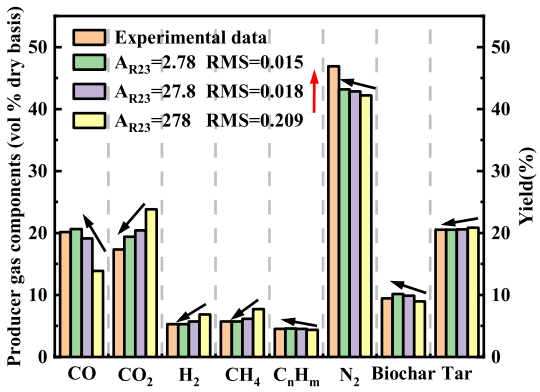

Fig. 3. The comparison results at different pre-exponential factor of R23 between prediction data and the experimental data under operating condition (ER = 0.12 and T = 673 °C).

$$Y_{0,ch} = 0.07 + 0.85\cdot\exp\left(-0.48\cdot10^{-2}\cdot T\right) \tag{5}$$

$$Y_{\mathrm{C,tar}} = \left(1.05 + 1.9\cdot10^{-4}\cdot T\right) \bullet Y_{\mathrm{C,F}} \tag{6}$$

$$Y_{0.\mathrm{tar}} = \left(0.92 - 2.2\cdot10^{-4}\cdot T\right) \bullet Y_{0.\mathrm{F}} \tag{7}$$

$$Y_{\mathrm{H,tar}} = 1 - Y_{\mathrm{C,tar}} - Y_{0.\mathrm{tar}} \tag{8}$$

$$Y_{\mathrm{CO,F}} = \left(3\cdot10^{-4} + \frac{0.0429}{1 + \left(\frac{T}{632}\right)^{-7.23}}\right)^{-1} \bullet Y_{\mathrm{H_2,F}} \tag{9}$$

$$Y_{\mathrm{CH_4,F}} = -2.18\cdot10^{-4} + 0.146\cdot Y_{\mathrm{CO,F}} \tag{10}$$

$$Y_{\mathrm{H_2,F}} = 1.145\cdot\left(1 - \exp\left(-0.11\cdot10^{-2}\cdot T\right)\right)^{9.384} \tag{11}$$

$$LHV_G = -6.23 + 2.47\cdot10^{-2}\cdot T \tag{12}$$

Where, $Y_{C,F}$, $Y_{H,F}$ and $Y_{O,F}$ refer to the element content of CHO in biomass respectively; $Y_{H_2,F}$, $Y_{CO,F}$, $Y_{CH_4,F}$, $Y_{C_2H_4,F}$, $Y_{CO_2,F}$, $Y_{H_2O,F}$, $Y_{tar,F}$ and $Y_{ch,F}$ are the yield of H_2, CO, CH_4, C_2H_4, CO_2, H_2O, tar and char in the pyrolysis process separately; $Y_{C,ch}$, $Y_{H,ch}$, $Y_{O,ch}$, $Y_{C,tar}$, $Y_{H,tar}$ and $Y_{O,tar}$ refer to the element content of CHO in char and element content of CHO in tar respectively; Y_{C,C_2H_4}, Y_{C,CH_4}, $Y_{C,CO}$, Y_{C,CO_2}, Y_{H,C_2H_4}, Y_{H,CH_4}, Y_{H,H_2O}, Y_{H,H_2}, $Y_{O,CO}$, Y_{O,CO_2} *and* Y_{O,H_2O} are the mass fraction of C in C_2H_4, CH_4, CO and CO_2, the mass fraction of H in C_2H_4, CH_4, H_2O and H_2, the mass fraction of O in CO, CO_2 and H_2O separately;

$$\begin{bmatrix} Y_{C,tar} & Y_{C,C_2H_4} & Y_{C,CH_4} & Y_{C,CO} & Y_{C,CO_2} & 0 & 0 \\ Y_{H,tar} & Y_{H,C_2H_4} & Y_{H,CH_4} & 0 & 0 & Y_{H,H_2O} & Y_{H,H_2} \\ Y_{O,tar} & 0 & 0 & Y_{O,CO} & Y_{O,CO_2} & Y_{O,H_2O} & 0 \\ 0 & 0 & 0 & -\Omega_1 & 0 & 0 & 1 \\ 0 & 0 & -1 & 0.146 & 0 & 0 & 0 \\ LHV_G & LHV_{C_2H_4} & LHV_{CH_4} & LHV_{CO} & 0 & LHV_G & LHV_{H_2} \\ 0 & 0 & 0 & 0 & 0 & 0 & 1 \end{bmatrix} \bullet \begin{bmatrix} Y_{tar,F} \\ Y_{C_2H_4,F} \\ Y_{CH_4,F} \\ Y_{CO,F} \\ Y_{CO_2,F} \\ Y_{H_2O,F} \\ Y_{H_2,F} \end{bmatrix} = \begin{bmatrix} Y_{C,F} - Y_{C,ch} \bullet Y_{ch,F} \\ Y_{H,F} - Y_{H,ch} \bullet Y_{ch,F} \\ Y_{O,F} - Y_{O,ch} \bullet Y_{ch,F} \\ 0 \\ 2.18 \bullet 10^{-4} \\ \left(\sum_i Y_{i,F} - Y_{ch,F} \bullet \sum_i Y_{i,ch}\right) \bullet LHV_G \\ \Omega_2 \end{bmatrix} \quad i = C, H, O \tag{1}$$

$$Y_{ch,F} = 0.106 + 2.43\cdot\exp\left(-0.66\cdot10^{-2}\cdot T\right) \tag{2}$$

$$Y_{C,ch} = 0.93 - 0.92\cdot\exp\left(-0.42\cdot10^{-2}\cdot T\right) \tag{3}$$

$$Y_{\mathrm{H},ch} = -0.41\cdot10^{-2} + 0.10\cdot\exp\left(-0.24\cdot10^{-2}\cdot T\right) \tag{4}$$

Table 3
Tar-related reactions and reaction kinetics.

Reaction		Reaction rate expression	Reference
R1	$C_3H_6O_2 \rightarrow 0.5C_6H_6O + 1.5H_2O$	$r = 3.00 \times 10^6 \exp\left(-\frac{136000}{RT}\right) C_{C_3H_6O_2}$	[26,28]
R2	$C_6H_6O \rightarrow CO + 0.4C_{10}H_8 + 0.15C_6H_6 + 0.1CH_4 + 0.75H_2$	$r = 3.20 \times 10^{11} \exp\left(-\frac{247000}{RT}\right) C_{C_6H_6O}$	[29]
R3	$C_{10}H_8 \rightarrow 6.05C + 0.4C_6H_6 + 1.25CH_4 + 0.15C_2H_4$	$r = 1.00 \times 10^7 \exp\left(-\frac{100000}{RT}\right) C_{C_{10}H_8}{}^{1.6} C_{H_2}{}^{-0.5}$	[11,28,30]
R4	$C_6H_6O + 4O_2 \rightarrow 6CO + 3H_2O$	$r = 655T \exp\left(-\frac{80200}{RT}\right) C_{C_6H_6O}{}^{0.5} C_{O_2}$	[11]
R5	$C_7H_8 + 3.5O_2 \rightarrow 7CO + 4H_2$	$r = 2.08 \times 10^9 T \exp\left(-\frac{165000}{RT}\right) C_{C_7H_8}{}^{0.5} C_{O_2}$	[31]
R6	$C_{10}H_8 + 5O_2 \rightarrow 10CO + 4H_2$	$r = 2.07 \times 10^4 T \exp\left(-\frac{80200}{RT}\right) C_{C_{10}H_8}{}^{0.5} C_{O_2}$	[31]
R7	$C_6H_6 + 4.5O_2 \rightarrow 6CO + 3H_2O$	$r = 2.40 \times 10^{11} \exp\left(-\frac{126000}{RT}\right) C_{C_6H_6}{}^{0.5} C_{O_2}$	[2,11]
R8	$C_6H_6O + 2H_2O \rightarrow 3CO + C_2H_4 + CH_4 + H_2$	$r = 1.00 \times 10^7 \exp\left(-\frac{100000}{RT}\right) C_{C_6H_6O}$	[11]
R9	$C_{10}H_8 + 2H_2O \rightarrow 3CH_4 + 2CO + 5C$	$r = 1.70 \times 10^{14} \exp\left(-\frac{350000}{RT}\right) C_{C_{10}H_8}{}^{1.6} C_{H_2}{}^{-0.5}$	[30,32]
R10	$C_7H_8 + H_2O \rightarrow C_6H_6 + CO + 2H_2$	$r = 1.00 \times 10^8 \exp\left(-\frac{100000}{RT}\right) C_{C_7H_8}$	[33,34]
R11	$C_7H_8 + H_2 \rightarrow C_6H_6 + CH_4$	$r = 1.04 \times 10^{12} \exp\left(-\frac{247000}{RT}\right) C_{C_7H_8} C_{H_2}{}^{0.5}$	[30,34,35]
R12	$C_6H_6 + 2H_2O \rightarrow 1.5C + 2CO + 2.5CH_4$	$r = 4 \times 10^{16} \exp\left(-\frac{443000}{RT}\right) C_{C_6H_6}{}^{1.3} C_{H_2}{}^{-0.4} C_{H_2O}{}^{0.2}$	[29]

$LHV_G(MJ/kg)$, $LHV_{C_2H_4}(MJ/kg)$, $LHV_{CH_4}(MJ/kg)$, $LHV_{CO}(MJ/kg)$ and $LHV_{H_2}(MJ/kg)$ refer to the lower heat value of the total pyrolysis gas, C_2H_4, CH_4, CO and H_2 respectively; $\Omega 1 = Y_{H_2,F}/Y_{CO,F}$, $\Omega 2 = Y_{H_2,F}$, T(°C) is the pyrolysis temperature.

2.3.2. Tar reaction and gasification reaction

In the simulation, it is assumed that tar is only composed of C, H and O elements, so the element content of carbon and oxygen in tar is determined by equation (6) and equation (7) in the pyrolysis model, while the element content of hydrogen in tar is calculated by the difference. According to the element content of carbon, hydrogen and oxygen in tar, tar is represented by $C_aH_bO_c$ and converted into a group of common representative compounds of tar during pyrolysis, among which $C_3H_6O_2$ represents primary tar. The specific conversion path is shown in equation (13) below, where x_1, x_2 and x_3 are determined by the elemental balance calculation of C, H and O [26]. Tar compounds in the pyrolysis process are produced and then undergo oxidation combustion and gasification reduction reaction with gaseous components in the reactor.

$$Y_{tar,F} \bullet C_aH_bO_c \underset{Pyrolysis}{\rightarrow} x_1 \bullet C_3H_6O_2 + x_2 \bullet C_7H_8 + x_3 \bullet H_2 \tag{13}$$

In order to determine the kinetic mechanism of biomass partial gasification for producer gas and biochar co-production in the bubbling fluidized bed based on our previous experimental data and evaluate the predictive effect of each reaction kinetic parameter considered in the model on the experimental results, the pre-exponential factor of the selected reactions from different literatures was modified [27]. For quantifying the error between the prediction results and the corresponding experimental results, the root mean square (RMS) value is used, the definition is shown in the following equation (14). Fig. 3 shows the comparison results at different pre-exponential factor of R23 between prediction data and the experimental data of poplar sawdust partial gasification for producer gas and biochar coproduction in the bubbling fluidized bed under operating condition (ER = 0.12 and T = 673 °C) [24]. The results suggest that the error is minimum when the pre-exponential factor is 2.78. Compared with the higher pre-exponential factor of R23, the lower pre-exponential factor of R23 can better predict the process of biomass partial gasification for producer gas and biochar co-production in the bubbling fluidized bed, which is more consistent with the kinetic mechanism of biomass partial gasification for producer gas and biochar co-production in the bubbling fluidized bed. The kinetic parameters of all chemical reactions used in the final model were determined by this method of observing the error direction and rationalization argument, which are shown in Tables 3 and 4.

$$RMS = \sqrt{\frac{\sum_{i-1}^{N} \left(Y_{i,\exp} - Y_{i,\sin}\right)^2}{N}} \tag{14}$$

2.4. Related index calculation

After the simulation, the relevant indexes are calculated based on the post-simulation results as follows:

(1) Air equivalence ratio(ER)

ER, which is the ratio of the input air flow in the simulation process of biomass partial gasification to the theoretical air required for the complete combustion, can be calculated by following equation:

$$\mathrm{ER} = \frac{V_{air}}{M_{biomass} \times \left(\frac{air}{biomass}\right)_{stoic}} \tag{15}$$

where, ER is the air equivalence ratio, V_{air} (Nm^3/h) is the volume flow rate of air, $M_{biomass}$ (kg/h) is the mass flow rate of biomass, and $(air/biomass)_{stoic}$ (Nm^3/kg) is the theoretical air required per unit mass.

(2) Gas production rate

Gas production rate, which is the volume of producer gas per unit mass of biomass under standard conditions, can be calculated by following equation:

$$G_v = \frac{V_{producer\ gas}}{M_{biomass}} \tag{16}$$

where: G_V (Nm^3/kg) is the gas production rate, and $V_{producer\ gas}$ (Nm^3/h) is the volume flow rate of producer gas.

(3) The lower heat value of producer gas

The lower heat value of producer gas, which is the chemical energy included in the per unit volume of producer gas, can be calculated by

Table 4
Gasification reactions and its reaction kinetics.

Reaction		Reaction rate expression	Reference
R13	$\alpha C(s) + O_2 \rightarrow 2(\alpha - 1)CO + (2 - \alpha)CO_2$	$r = 29.8T \exp\left(-\frac{149000}{RT}\right)\frac{6}{d_p}C_{O_2}\ \alpha = \frac{1+2f}{1+f}$ with $f = 4.72 \times 10^{-3} \exp\left(-\frac{37787}{RT}\right)$	[11,36]
R14	$CO + 0.5O_2 \rightarrow CO_2$	$r = 2.32 \times 10^{12} \exp\left(-\frac{167000}{RT}\right) C_{CO}{C_{O_2}}^{0.25}{C_{H_2O}}^{0.5}$	[2]
R15	$CH_4 + 0.5O_2 \rightarrow CO + 2H_2$	$r = 1.58 \times 10^{12} \exp\left(-\frac{202000}{RT}\right) {C_{CH_4}}^{0.7}{C_{O_2}}^{0.8}$	[11]
R16	$C_2H_4 + 3O_2 \rightarrow 2CO_2 + 2H_2O$	$r = 3.552 \times 10^{11} \exp\left(-\frac{130529}{RT}\right) C_{C_2H_4}C_{O_2}$	[37]
R17	$H_2 + 0.5O_2 \rightarrow H_2O$	$r = 2.196 \times 10^{9} \exp\left(-\frac{28517}{RT}\right) C_{H_2}C_{O_2}$	[29]
R18	$C + H_2O \rightarrow H_2 + CO$	$r = \frac{k_1 P_{H_2O}}{1 + k_2 P_{H_2O} + k_3 P_{H_2}}$ $k_1 = 4.93 \times 10^{3} \exp\left(\frac{-18522}{T}\right)$ $k_2 = 1.1 \times 10^{1} \exp\left(\frac{-3548}{T}\right)$ $k_3 = 1.53 \times 10^{-9} \exp\left(\frac{25161}{T}\right)$	[29]
R19	$C + CO_2 \rightarrow 2CO$	$r = 4.364 \times 10^{3} \exp\left(-\frac{248123}{RT}\right) C_{CO_2}$	[29]
R20	$C + 2H_2 \rightarrow CH_4$	$r = 1.29 \exp\left(-\frac{19210}{RT}\right) C_{H_2}$	[38,39]
R21	$CH_4 + H_2O \rightarrow CO + 3H_2$	$r = 3.00 \times 10^{8} \exp\left(-\frac{125000}{RT}\right) C_{CH_4}C_{H_2O}$	[2,40]
R22	$C_2H_4 + 2H_2O \rightarrow 2CO + 4H_2$	$r = 3.00 \times 10^{8} \exp\left(-\frac{125000}{RT}\right) C_{C_2H_4}{C_{H_2O}}^2$	[41,42]
R23	$CO + H_2O \rightarrow CO_2 + H_2$	$r = 2.78 \exp\left(-\frac{12600}{RT}\right)\left(C_{CO}C_{H_2O} - \frac{C_{H_2}C_{CO_2}}{K_{EQ}}\right)$ $K_{EQ} = 0.022 \exp\left(\frac{34730}{RT}\right)$	[11]
R24	$CO_2 + H_2 \rightarrow CO + H_2O$	$r = 3.20 \times 10^{8} \exp\left(-\frac{164200}{RT}\right) C_{CO_2}{C_{H_2}}^{0.33}$	[43,44]

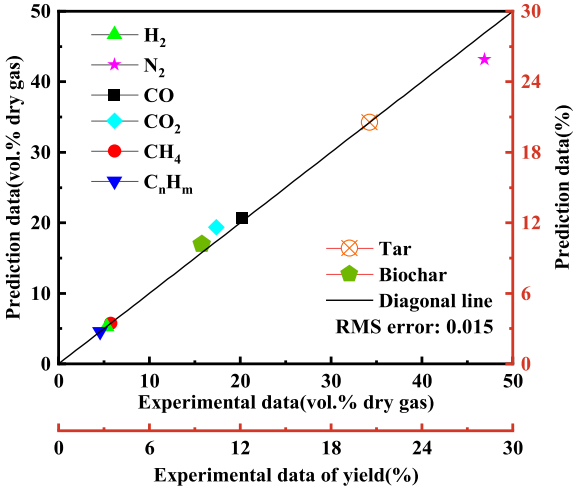

Fig. 4. Comparison between prediction results of kinetic model for biomass partial gasification and experimental results under operating condition (ER = 0.12, T = 673 °C).

following equation:

$$LHV_{producer\ gas} = 12.64X_{CO} + 10.79X_{H_2} + 35.88X_{CH_4} + 59.44X_{C_2H_4} \quad (17)$$

where: $LHV_{producer\ gas}$ (MJ/Nm^3) is the lower heat value of producer gas, and X_j is the mole fraction of combustible components j (CO, H_2, CH_4, C_2H_4) in producer gas.

(4) Gasification efficiency

Gasification efficiency, which is the ratio of the chemical energy included in the producer gas to the chemical energy included in the biomass feeding in the same time, can be calculated as follows:

$$\psi = \frac{LHV_{producer\ gas} \times V_{producer\ gas}}{M_{biomass} \times LHV_{biomass}} \quad (18)$$

where, ψ represents the gasification efficiency and $LHV_{biomass}$ (MJ/kg) represents the lower heat value of biomass.

(5) Carbon conversion ratio

The carbon conversion ratio of biomass partial gasification simulation process, which is the proportion of carbon in biomass converted to producer gas and tar, can be calculated as follows:

$$\eta_C = 1 - \frac{M_{biochar} \times C_{biochar}}{M_{biomass} \times C_{biomass}} \quad (19)$$

where: η_C is the carbon conversion ratio, $M_{biochar}$ (kg/h) is the biochar output, $C_{biochar}$ (%) is the carbon content of biochar, and $C_{biomass}$ (%) is the carbon content of biomass.

3. Results and discussion

3.1. Model validation

In order to verify the rationality and accuracy of the finally established kinetic model of biomass partial gasification for producer gas and biochar coproduction in the bubbling fluidized bed, the prediction results of the model were compared with the experimental results of partial gasification for producer gas and biochar coproduction in the bubbling fluidized bed. Fig. 4 shows the comparison results between

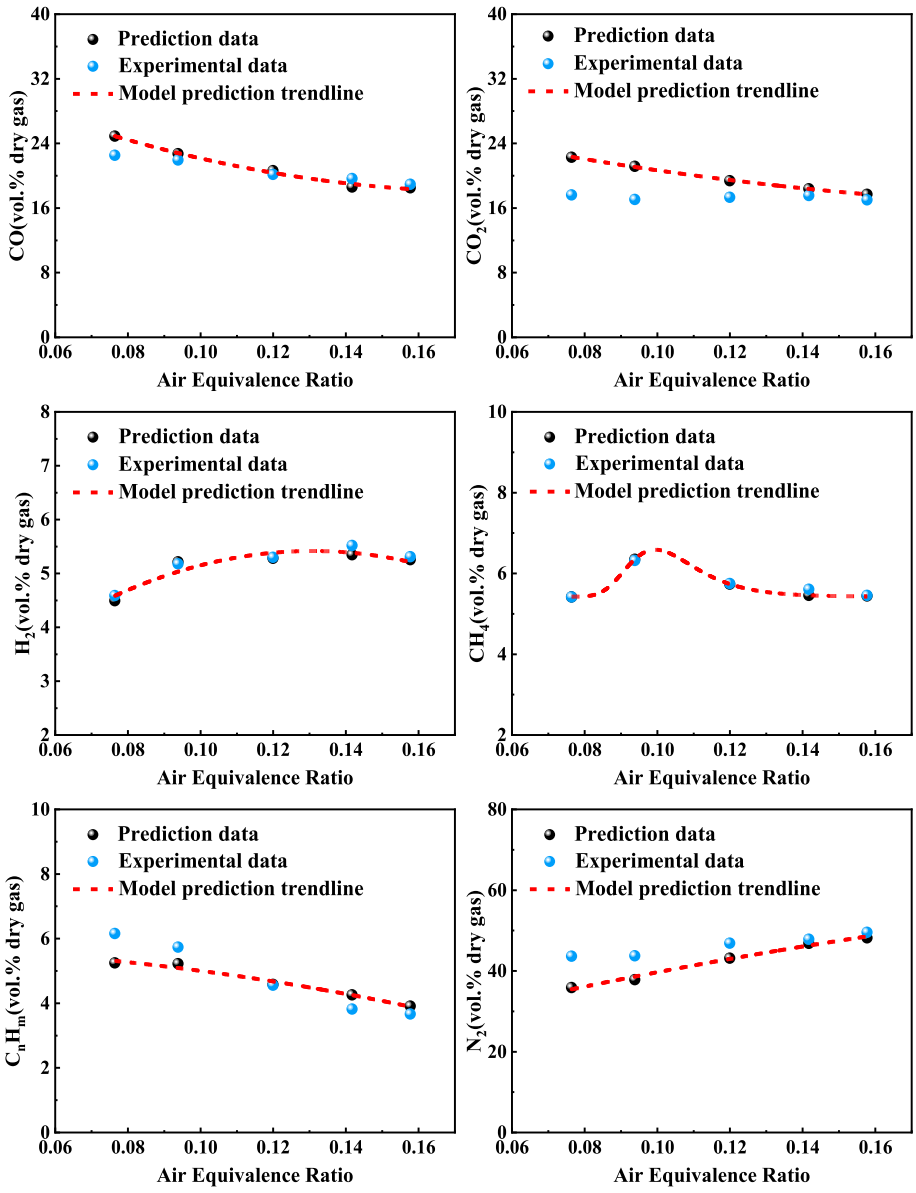

Fig. 5. Comparison of model prediction results with experimental results of at different air equivalence ratios for the producer gas components (vol % dry basis).

prediction data of the kinetic model of biomass partial gasification for producer gas and biochar coproduction in the bubbling fluidized bed and the experimental data of poplar sawdust partial gasification for producer gas and biochar coproduction in the bubbling fluidized bed under operating condition (ER = 0.12 and T = 673 °C). The results show that the error between the model prediction results and the corresponding experimental results is small, the prediction performance of model is good, and the model can accurately predict the producer gas components, biochar yield and tar yield in the process of biomass partial gasification for producer gas and biochar coproduction in the bubbling fluidized bed.

3.2. *Effect of ER on the characteristics of biomass partial gasification for producer gas and biochar co-production*

In the actual operation process of industrial biomass gasification plant, the gasification temperature is determined by regulating the air equivalence ratio and has a one-to-one corresponding relationship with the air equivalence ratio. Therefore, in order to test the robustness of the established kinetic model of biomass partial gasification for producer gas and biochar in the bubbling fluidized bed, the model prediction results under different air equivalence ratios with the experimental results under the same conditions [24] will be comprehensively compared for the whole products of biomass partial gasification in this section.

3.2.1. *Effect of ER on producer gas composition and gasification performance*

Fig. 5 shows the comparison between the model prediction data of biomass partial gasification in the bubbling fluidized bed under different air equivalence ratios and the experimental data of poplar sawdust partial gasification under the same conditions for the producer gas components. The results indicate that the model prediction data is in good agreement with the experimental data. With the increase of the air equivalence ratio and gasification temperature, both the volume content of CO and CO_2 in the model prediction data continue to decline, and it is worth mentioning that the volume content and the decreasing rate of CO are larger than CO_2. For CO, on the one hand, it mostly produced by exothermic reaction R13 [45], the increase of air equivalence ratio and the gasification temperature make the reaction equilibrium shift to the left, which is not conducive to the generation of CO. On the other hand,

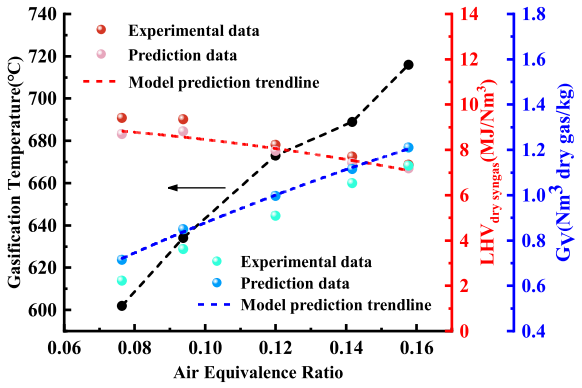

Fig. 6. Comparison of model prediction results with experimental results at different air equivalence ratios for gas production rate and lower calorific value of producer gas.

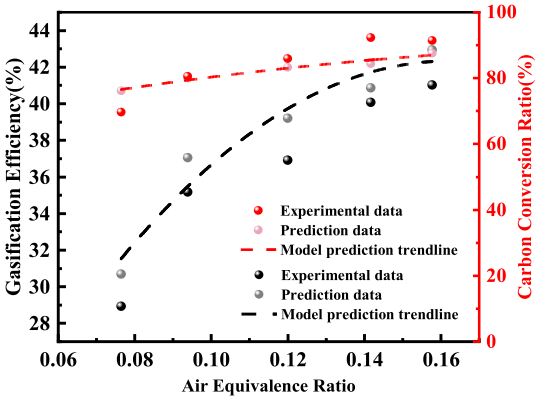

Fig. 7. Comparison of model prediction results with experimental results at different air equivalence ratios for gasification efficiency and carbon conversion ratio.

the increase of air equivalence ratio and gasification temperature also promote the reaction rate of combustion reaction R14, resulting in the increase of CO consumption. As for CO_2, on the one hand, the rise of temperature causes the reaction rate of exothermic reaction R13 to decrease, which prevents the generation of CO_2; on the other hand, the rise of temperature leads to the increase of the reaction rate of combustion reaction R14, resulting in the rise of CO_2, and reduction reaction R19 is limited by the complex heat transfer at low temperatures, which is the reason why the falling rate of CO is larger than CO_2 in the simulated data. At the same time, due to the lower air equivalence ratio investigated in the simulation process, the degree of partial combustion of biomass into CO is greater, which leads to the volume content of CO is larger than CO_2.

For H_2, with the increase of air equivalence ratio, the volume content of H_2 shows an increasing-decreasing trend. On the one hand, the rise of air equivalence ratio and the gasification temperature shift the steam reforming reaction equilibrium to the right, which is favorable to the generation of H_2; on the other hand, when the air equivalence ratio and gasification temperature increase to a certain extent, the combustion reaction rate of H_2 is greatly enhanced, and the volume content of H_2 declines. For CH_4, with the rise of air equivalence ratio, the volume content of CH_4 also presents a trend of increasing-decreasing, but the turning point is different from H_2, which is due to CH_4 mainly comes from the pyrolysis of biomass and the decomposition of hydrocarbons [45].

For hydrocarbon C_nH_m, with the increase of air equivalence ratio, the volume content of C_nH_m shows a descending trend. On the one hand, C_nH_m mainly derives from the pyrolysis of biomass, and the rise of

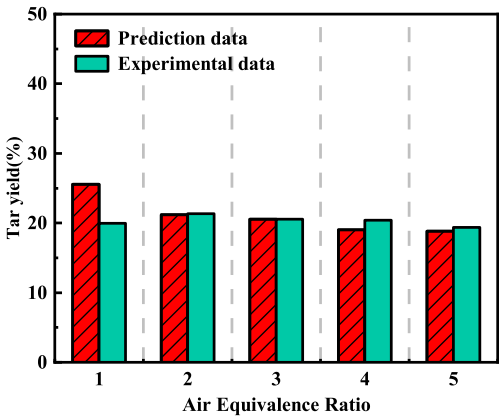

Fig. 8. Comparison of model prediction results with experimental results at different air equivalence ratios for tar yield.

gasification temperature promotes its yield to rise. Meanwhile, the decomposition of tar also contributes to the generation of C_nH_m [46], but due to the low temperature under study, its production degree is limited; On the other hand, with the rise of air equivalence ratio and temperature, the reaction rate of combustion reaction R16 and steam reforming reaction R22 continue to go up, promoting the consumption of C_nH_m. Under the interaction of these two aspects, the volume content of C_nH_m continues to decrease macroscopically. For N_2, with the increase of air equivalence ratio, the volume content of N_2 continues to rise, mainly because the producer gas production rate is low at the lower air equivalence ratio, and the introduction effect of N_2 keeps increase with the rise of air equivalence ratio. These results are consistent with results reported in the literature [11,47].

Fig. 6 gives the comparison between the model prediction data of partial gasification in bubbling fluidized bed under different air equivalence ratios and the experimental data of poplar sawdust partial gasification in the bubbling fluidized bed under the same condition for gas production rate and lower calorific value of producer gas, and the results suggest that the model prediction data and the experimental data of gas production rate present the increasing trend with the rise of the air equivalence ratio, which is in accordance with results [48]. The reason is that the increase of air equivalence ratio and gasification temperature is advantageous to the gasification reaction. And it is worth noting that the model prediction data are larger than the experimental data, which is mainly due to the more ideal reaction conditions during the simulation. The prediction data and experimental data of lower calorific value of producer gas are decreasing with the increase of air equivalence ratio, and the error between the data decreases gradually, which is mainly due to the fact that the introduction effect of N_2 enhances the dilution of volume content of combustible gases in the producer gas with the rise of the air equivalence ratio.

Fig. 7 gives the comparison between the model prediction data of gasification efficiency and carbon conversion ratio from partial gasification in bubbling fluidized bed under different air equivalence ratios and the experimental data of poplar sawdust partial gasification in the bubbling fluidized bed under the same condition, which demonstrates that the model prediction data and the experimental data of gasification efficiency and carbon conversion ratioare in good agreement and the change trend is consistent, and both of them show the rising trend with the increase of air equivalence ratio. The reason is that the increase of air equivalence ratio and gasification temperature is beneficial to the gasification reaction, the rapid precipitation of volatiles in biomass and the partial combustion of fixed carbon, so that more carbon in biomass can be converted into gas and liquid products. At the same time, it is worth noting that the increase rates of gasification efficiency and carbon conversion ratio in both model prediction data and experimental data drop with the increase of air equivalence ratio, which directly verifies

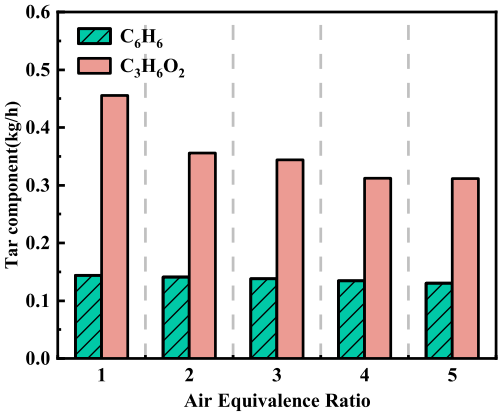

Fig. 9. Variation law of production output for main tar components in prediction results.

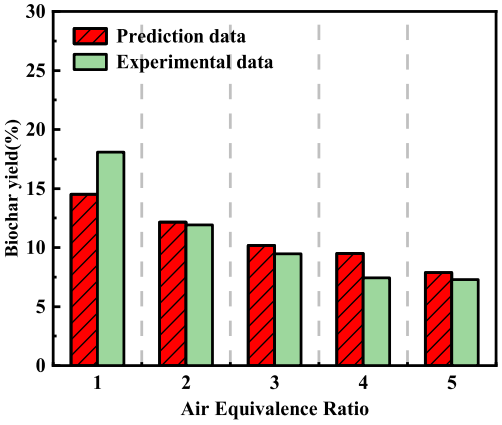

Fig. 10. Comparison of model prediction results with experimental results at different air equivalence ratios for biochar yield.

Table 5
Ultimate analysis and Proximate analysis of biochar in model prediction results under different air equivalent ratios.

Items	Ultimate analysis/(wt%)					Proximate analysis/(wt%)		
	C_d	H_d	N_d	$S_{t,d}$	O_d	A_d	V_d	FC_d
1	79.16	1.73	0.69	0.26	9.00	9.15	23.61	67.24
2	79.16	1.73	0.59	0.30	7.29	10.93	18.72	70.35
3	79.15	1.67	0.50	0.34	5.28	13.06	14.12	72.82
4	78.87	1.60	0.49	0.35	4.70	13.99	12.67	73.34
5	75.93	1.70	0.56	0.41	4.56	16.85	10.78	72.37

Note: d: dry basis.

the feasibility of biomass partial gasification. These results are consistent with results reported in the literature [49].

3.2.2. Effect of ER on tar characteristic

Fig. 8 shows the comparison between the model prediction data of tar yield from partial gasification in the bubbling fluidized bed under different air equivalence ratios and the experimental data of poplar sawdust partial gasification in bubbling fluidized bed under the same working conditions, in which the working conditions under study are marked as 1, 2, 3, 4, and 5, respectively, according to the air equivalence ratio from small to large in the following part of the figure. The results manifest that the errors between the model prediction data and the experimental data of tar yield are relatively small and the variation trends of data are inconsistent. The model prediction data show a decreasing trend with the increase of air equivalence ratio, while the experimental data present an increasing-decreasing trend, the only difference is at the lowest air equivalence ratio studied, which is due to the fact that the higher the air equivalence ratio and the gasification temperature, the smaller the gap between the simulative and experimental reaction conditions, and the smaller the error between prediction data and experimental data. As for the decrease in tar yield, it is mainly owing to the fact that the rise of air equivalence ratio and gasification temperature contributes to the oxidation reaction and secondary decomposition of the tar components, which can be confirmed by the continuous decrease of production output for primary tar $C_3H_6O_2$ and stable component C_6H_6 among the main tar components in the simulation results of Fig. 9.

Table 6
Regression equation for total product and gasification performance index of biomass partial gasification.

Items		Regression equation	R^2
Gaseous product	CO	626.75*(ER^2)-227.34*ER+38.61	0.99
	CO_2	231.13*(ER^2)-111.02*ER+29.46	0.99
	CH_4	5.43 + 1.16*exp(-exp(-z)-z+1) z=(ER-0.10)/0.01	0.99
	H_2	−282.28*(ER^2)+73.80*ER+0.59	0.95
	C_nH_m	−74.78*(ER^2)+0.07*ER+5.74	0.98
	N_2	−313.04*(ER^2)+234.33*ER+19.39	0.99
Liquid product	Tar	19.05 + 361.26*(1.19E-23^ER)	0.96
Solid product	Biochar	443.68*(ER^2)-178.86*ER+25.37	0.98
ψ		−1479.94*(ER^2)+479.07*ER+3.56	0.95
η_C		−546.45*(ER^2)+256.19*ER+60.18	0.97

3.2.3. Effect of ER on biochar characteristic

Fig. 10 presents the comparison between the prediction data of biochar yield from partial gasification in the bubbling fluidized bed under different air equivalence ratios and the experimental data of poplar sawdust partial gasification under the same working conditions. The results suggest that the prediction data of the biochar yield is in good agreement with the experimental data, the change trend is consistent, and both of them decrease with the increase of air equivalence ratio. This is mainly because the increase of air equivalence ratio and gasification temperature contributes to the reaction of biomass particles with oxygen, the precipitation of more volatile components and the reaction of fixed carbon.

Table 5 shows the changes for ultimate and proximate analysis of biochar in the prediction results of model under different air equivalence ratios, in which the volatiles fraction is determined based on the fitting data of the volatiles residual rate in biochar obtained from experiments under different air equivalence ratios. The results show that with the increase of air equivalence ratio, the carbon content in biochar decreases from 79.16 % to 75.93 %, volatiles fraction drops from 23.61 % to 10.78 %. The main reason is that the increase of air equivalence ratio leads to the increase of gasification temperature, the acceleration precipitation of volatiles and the increase of the combustion share for fixed carbon.

3.3. Regression analysis

In order to consolidate the simulation results of the kinetic model of biomass partial gasification for producer gas and biochar cogeneration in the fluidized bed, regression analysis was performed on the correlation between the full products and gasification performance indexes of biomass partial gasification and the air equivalence ratio, the correlation applies to the air equivalent ratio range of 0.07–0.16, and the temperature range of 602°C–716 °C. The correlation between the full products and the gasification performance indexes of biomass partial gasification and the air equivalence ratio is specifically see Table 6.

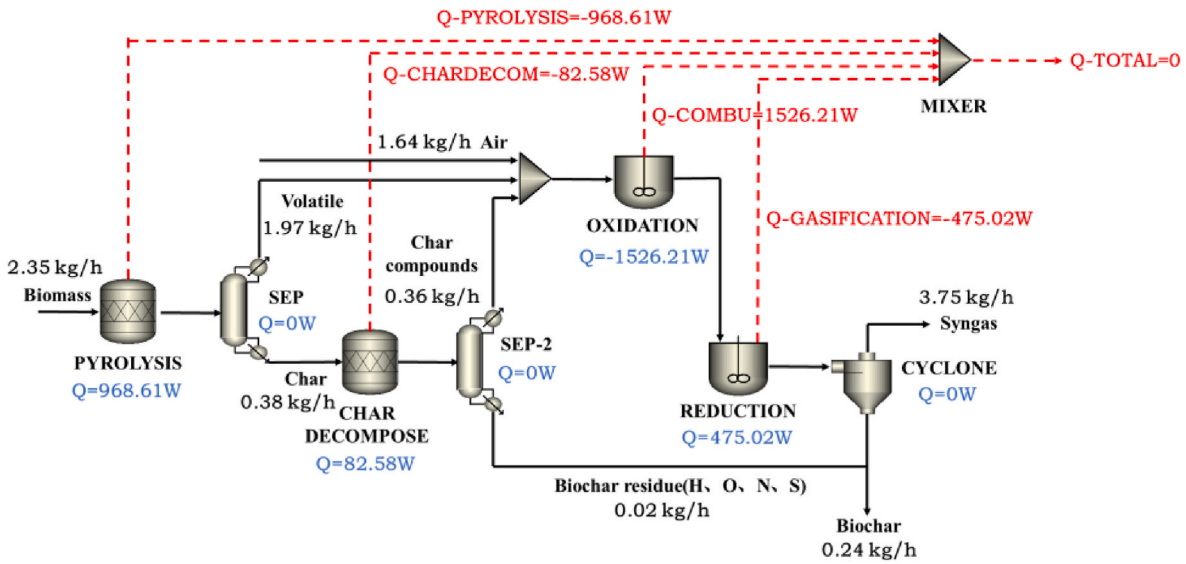

Fig. 11. Mass flow and energy flow of biomass partial gasification in bubbling fluidized bed under operating condition (ER = 0.12, T = 673 °C).

Table 7
Energy flow of biomass partial gasification in bubbling fluidized bed under different air equivalence ratios.

Operating condition	Biomass pyrolysis	Char pyrolysis	Reduction	Oxidation
1	806.40W	102.94W	356.05W	−1265.39W
2	878.22W	88.17W	420.06W	−1386.46W
3	968.61W	82.58W	475.02W	−1526.21W
4	1010.07W	80.02W	493.30W	−1583.40W
5	1091.92W	71.92W	547.63W	−1711.47W

3.4. Effect of ER on energy balance

Energy balance is very important in the kinetic simulation process of biomass partial gasification for producer gas and biochar in bubbling fluidized bed. Therefore, in order to test the rationality of the established kinetic model of biomass partial gasification for producer gas and biochar in bubbling fluidized bed, the energy balance in the pyrolysis stage, oxidation combustion stage and gasification reduction stage of biomass partial gasification in bubbling fluidized bed are evaluated in this section.

Fig. 11 shows the mass flow and energy flow simulation data of biomass partial gasification in bubbling fluidized bed under operating condition(ER = 0.12, T = 673 °C). The results reveal that both the pyrolysis stage and gasification stage are endothermic processes, while the oxidation combustion stage is exothermic process, and the oxidation combustion stage acts as the heat source in the whole process of biomass partial gasification in bubbling fluidized bed. The heat released in the oxidation combustion stage is 1526.21W, the heat absorbed in the pyrolysis stage is 1051.19W, and the heat absorbed in the gasification reduction stage is 475.02W. In order to evaluate the influence of air equivalence ratio on energy balance during the process of biomass partial gasification for producer gas and biochar in bubbling fluidized bed, the absorbing heat in the pyrolysis process and the gasification reduction process and the releasing heat in the oxidation combustion process under different air equivalence ratios are calculated, and the results are shown in Table 7. The results show that with the increase of air equivalence ratio, the absorbing heat of pyrolysis process and gasification reduction process increase, and the releasing heat of oxidation combustion process also rise. The reason is that the rise of air equivalence ratio helps to increase the oxidation share of biomass particles and enhance the rate of related oxidative exothermic reaction, thus increasing the releasing heat in oxidation combustion process, which is the reason for the rise of gasification temperature in Fig. 6. The rise of temperature promotes the rate of endothermic reaction in gasification reduction stage, resulting in the increase of the absorbing heat in gasification reduction process. And the higher the temperature, the more heat absorbing in the pyrolysis stage for the same reason.

4. Conclusion

In this paper, Aspen plus was used to establish a kinetic model of biomass partial gasification for producer gas and biochar coproduction in bubbling fluidized bed with tar reaction kinetics and biochar elements distribution in consideration, the model were verified by relevant experimental data and the energy balance in the pyrolysis stage, oxidation stage and reduction stage of biomass partial gasification process in the bubbling fluidized bed was evaluated. The results demonstrate that this model can well predict the producer gas components, biochar, gasification efficiency, carbon conversion ratio and their change trends in the partial gasification process in bubbling fluidized bed under different air equivalence ratios. The prediction results are as follows: With the increase of air equivalence ratio(from 0.07 to 0.16), the gasification temperature keeps rising(from 602 °C to 716 °C), the volume contents of CO, CO_2 and C_nH_m decrease continuously, the volume contents of H_2 and CH_4 show an increasing-decreasing trend, but with different turning points, and the volume content of N_2 increase continuously; tar yield decreases; biochar yield continues to decline, the carbon and oxygen content in biochar decrease continuously, and the ash content and volatile content also drop continuously; the gasification efficiency and carbon conversion ratio increase, but the decreasing rate decreases, which verified the feasibility of biomass partial gasification; the heat absorbing from the oxidation stage in the pyrolysis stage and reduction stage increase, and the releasing heat in oxidation stage also rise. The model has the potential to predict the process of different biomass partial gasification for producer gas and biochar coproduction in bubbling fluidized bed.

CRediT authorship contribution statement

Deao Zhu: Writing – original draft, Methodology, Formal analysis, Data curation. **Qinhui Wang:** Writing – review & editing, Funding acquisition, Conceptualization. **Zijun Zhang:** Writing – review & editing, Investigation. **Guilin Xie:** Project administration, Investigation. **zhongyang Luo:** Writing – review & editing, Funding acquisition.

Declaration of competing interest

The authors declare that they have no known competing financial interests or personal relationships that could have appeared to influence the work reported in this paper.

Acknowledgements

This work was supported by the R&D Project of the Leading talents of Zhejiang Province – R&D and Demonstration application of resource and energy utilization technology for biochar and producer gas coproduction based on bamboo (2023C03174) and the Fundamental Scientific Research Funds for the Central Universities (2022ZFJH004).

Data availability

The authors do not have permission to share data.

References

[1] You S, Ok YS, Chen SS, Tsang DCW, Kwon EE, Lee J, Wang CH. A critical review on sustainable biochar system through gasification: energy and environmental applications. Bioresour Technol 2017;246:242–53.
[2] Gómez-Barea A, Leckner B. Modeling of biomass gasification in fluidized bed. Prog Energy Combust Sci 2010;36(4):444–509.
[3] Silva IP, Lima RMA, Silva GF, Ruzene DS, Silva DP. Thermodynamic equilibrium model based on stoichiometric method for biomass gasification: a review of model modifications. Renew Sustain Energy Rev 2019;114.
[4] Begum S, Rasul M, Akbar D, Ramzan N. Performance analysis of an integrated fixed bed gasifier model for different biomass feedstocks. Energies 2013;6(12):6508–24.
[5] K T AA, P S, C M, P A. Aspen plus simulation of biomass gasification: a comprehensive model incorporating reaction kinetics, hydrodynamics and tar production. Process Integration and Optimization for Sustainability 2022;7(1–2):255–68.
[6] Kartal F, Sezer S, Özveren U. Investigation of steam and CO2 gasification for biochar using a circulating fluidized bed gasifier model in Aspen HYSYS. J CO2 Util 2022;62.
[7] Cardoso J, Silva V, Eusébio D, Brito P, Boloy RM, Tarelho L, Silveira JL. Comparative 2D and 3D analysis on the hydrodynamics behaviour during biomass gasification in a pilot-scale fluidized bed reactor. Renew Energy 2019;131:713–29.
[8] Cardoso J, Silva V, Eusébio D, Brito P, Hall MJ, Tarelho L. Comparative scaling analysis of two different sized pilot-scale fluidized bed reactors operating with biomass substrates. Energy 2018;151:520–35.
[9] Couto ND, Silva VB, Monteiro E, Rouboa A. Assessment of municipal solid wastes gasification in a semi-industrial gasifier using syngas quality indices. Energy 2015;93:864–73.
[10] Saiful Alam M, Wijayanta AT, Nakaso K, Fukai J. Study on coal gasification with soot formation in two-stage entrained-flow gasifier. International Journal of Energy and Environmental Engineering 2015;6(3):255–65.
[11] Puig-Gamero M, Pio DT, Tarelho LAC, Sánchez P, Sanchez-Silva L. Simulation of biomass gasification in bubbling fluidized bed reactor using aspen plus®. Energy Convers Manag 2021;235.
[12] Mutlu ÖÇ, Zeng T. Challenges and opportunities of modeling biomass gasification in aspen plus: a review. Chem Eng Technol 2020;43(9):1674–89.
[13] Tian Y, Du J, Luo Z, He D, Ma W, Zhou X, Liang S, Yuan L. Kinetic study on biomass gasification coupled with tar reforming for syngas production. Biomass Conversion and Biorefinery 2024;14:28377–85.
[14] Pio DT, Tarelho LAC. Empirical and chemical equilibrium modelling for prediction of biomass gasification products in bubbling fluidized beds. Energy 2020;202.
[15] Safarian S, Unnþórsson R, Richter C. A review of biomass gasification modelling. Renew Sustain Energy Rev 2019;110:378–91.
[16] Damartzis T, Michailos S, Zabaniotou A. Energetic assessment of a combined heat and power integrated biomass gasification–internal combustion engine system by using Aspen Plus®. Fuel Process Technol 2012;95:37–44.
[17] Kaushal P, Tyagi R. Advanced simulation of biomass gasification in a fluidized bed reactor using ASPEN PLUS. Renew Energy 2017;101:629–36.
[18] Li W, Wang C, Song Y. Simulation of waste tire gasification in bubbling fluidized bed by Aspen: contribution ratio analysis. Renew Energy 2024;222.
[19] Zhang Y, Ma H, Chen D, Zhou J. Technical and benefit evaluation of fruit-wood waste gasification heating coproduction of an activated carbon system. ACS Omega 2021;6(1):633–41.
[20] Xie Y, Wang L, Li H, Westholm LJ, Carvalho L, Thorin E, Yu Z, Yu X, Skreiberg Ø. A critical review on production, modification and utilization of biochar. J Anal Appl Pyrolysis 2022;161.
[21] Tauqir W, Zubair M, Nazir H. Parametric analysis of a steady state equilibrium-based biomass gasification model for syngas and biochar production and heat generation. Energy Convers Manag 2019;199.
[22] Yao Z, You S, Ge T, Wang C-H. Biomass gasification for syngas and biochar co-production: energy application and economic evaluation. Appl Energy 2018;209:43–55.
[23] Zhou Y. Experimental and Aspen Plus modeling research on bio-char and syngas co-production by gasification of biomass waste: the products and reaction energy balance evaluation. Biomass Conversion and Biorefinery 2023;14(4):5387–98.
[24] Zhu D, Wang Q, Xie G, Ye Z, Zhu Z, Ye C. Effect of air equivalence ratio on the characteristics of biomass partial gasification for syngas and biochar co-production in the fluidized bed. Renew Energy 2024;222.
[25] Neves D, Thunman H, Matos A, Tarelho L, Gómez-Barea A. Characterization and prediction of biomass pyrolysis products. Prog Energy Combust Sci 2011;37(5):611–30.
[26] Pauls JH, Mahinpey N, Mostafavi E. Simulation of air-steam gasification of woody biomass in a bubbling fluidized bed using Aspen Plus: a comprehensive model including pyrolysis, hydrodynamics and tar production. Biomass Bioenergy 2016;95:157–66.
[27] Alam MS, Wijayanta AT, Nakaso K, Fukai J. Sensitivity analysis of coal gasification in two-stage entrained-flow gasifier: syngas and carbon conversion prediction. J Therm Eng 2017;6:1574–87.
[28] Morf P, Hasler P, Nussbaumer T. Mechanisms and kinetics of homogeneous secondary reactions of tar from continuous pyrolysis of wood chips. Fuel 2002;81:843–53.
[29] Rafati M, Hashemisohi A, Wang L, Shahbazi A. Sequential modular simulation of hydrodynamics and reaction kinetics in a biomass bubbling fluidized-bed gasifier using aspen plus. Energy & Fuels 2015;29(12):8261–72.
[30] Jess A. Mechanisms and kinetics of thermal reactions of aromatic hydrocarbons from pyrolysis of solid fuels. Fuel 1996;75:1441–8.
[31] Ahmed AMA, Salmiaton A, Choong TSY, Wan Azlina WAKG. Review of kinetic and equilibrium concepts for biomass tar modeling by using Aspen Plus. Renew Sustain Energy Rev 2015;52:1623–44.
[32] Beheshti SM, Ghassemi H, Shahsavan-Markadeh R. Process simulation of biomass gasification in a bubbling fluidized bed reactor. Energy Convers Manag 2015;94:345–52.
[33] Taralas G, Kontominas MG, Kakatsios X. Modeling the thermal destruction of toluene (C_7H_8) as tar-related species for fuel gas cleanup. Energy & Fuels 2003;17:329–37.
[34] Du Y, Liu H, Ren W. Numerical investigations of a fluidized bed biomass gasifier coupling detailed tar generation and conversion kinetics with particle-scale hydrodynamics. Energy & Fuels 2020;34(7):8440–51.
[35] Heineken W, Cuesta DDL, Zobel N. Modeling tar recirculation in biomass fluidized bed gasification. Energy & Fuels 2016;30(4):3113–29.
[36] Champion WM, Cooper CD, Mackie KR, Cairney P. Development of a chemical kinetic model for a biosolids fluidized-bed gasifier and the effects of operating parameters on syngas quality. J Air Waste Manag Assoc 2014;64(2):160–74.
[37] Xie J, Zhong W, Jin B, Shao Y, Liu H. Simulation on gasification of forestry residues in fluidized beds by Eulerian-Lagrangian approach. Bioresour Technol 2012;121:36–46.
[38] Dhrioua M, Ghachem K, Hassen W, Ghazy A, Kolsi L, Borjini MN. Simulation of biomass air gasification in a bubbling fluidized bed using aspen plus: a comprehensive model including tar production. ACS Omega 2022;7(37):33518–29.
[39] Kumar U, Paul MC. CFD modelling of biomass gasification with a volatile break-up approach. Chem Eng Sci 2019;195:413–22.
[40] Duterque J, Borghi R, Tichtinsky H. Study of quasi-global schemes for hydrocarbon combustion. Combust Sci Technol 2007;26(1–2):1–15.
[41] Eri Q, Peng J, Zhao X. CFD simulation of biomass steam gasification in a fluidized bed based on a multi-composition multi-step kinetic model. Appl Therm Eng 2018;129:1358–68.
[42] Umeki K, Yamamoto K, Namioka T, Yoshikawa K. High temperature steam-only gasification of woody biomass. Appl Energy 2010;87(3):791–8.
[43] Abdelouahed L, Authier O, Mauviel G, Corriou JP, Verdier G, Dufour A. Detailed modeling of biomass gasification in dual fluidized bed reactors under aspen plus. Energy & Fuels 2012;26(6):3840–55.
[44] Bustamante F, Enick RM, Cugini AV, Killmeyer RP, Howard BH, Rothenberger KS, Ciocco MV, Morreale BD, Chattopadhyay S, Shi S. High-temperature kinetics of the homogeneous reverse water–gas shift reaction. AIChE J 2004;50(5):1028–41.
[45] Cheng J. Experimental research on typical biomass gasification characteristics in a circulated fluidized bed[D]. Hangzhou: Zhejiang University; 2019.
[46] Dun Q, Chen Z, Huang F, Zhou Y, Yu J, Gao S, et al. Influences of temperature and residence time on secondary reactions of volatiles from coal pyrolysis. Chin J Process Eng 2018;18:140–7.
[47] Gu H, Tang Y, Yao J, Chen F. Study on biomass gasification under various operating conditions. J Energy Inst 2019;92(5):1329–36.
[48] Pio DT, Tarelho LAC, Matos MAA. Characteristics of the gas produced during biomass direct gasification in an autothermal pilot-scale bubbling fluidized bed reactor. Energy 2017;120:915–28.
[49] Zhang X, Li H, Liu L, Bai C, Wang S, Zeng J, Liu X, Li N, Zhang G. Thermodynamic and economic analysis of biomass partial gasification process. Appl Therm Eng 2018;129:410–20.